

## A New Look at Pulsar Statistics—Birthrate and Evidence for Injection

M. Vivekanand and R. Narayan *Raman Research Institute,  
Bangalore 560080*

Received 1981 July 3; accepted 1981 September 30

**Abstract.** We make a statistical analysis of the periods  $P$  and period-derivatives  $\dot{P}$  of pulsars using a model independent theory of pulsar flow in the  $P$ – $\dot{P}$  diagram. Using the available sample of  $P$  and  $\dot{P}$  values, we estimate the current of pulsars flowing unidirectionally along the  $P$ -axis, which is related to the pulsar birthrate. Because of radio luminosity selection effects, the observed pulsar sample is biased towards low  $P$  and high  $\dot{P}$ . We allow for this by weighting each pulsar by a suitable scale factor. We obtain the number of pulsars in our galaxy to be  $6.05^{+3.32}_{-2.80} \times 10^5$  and the birthrate to be  $0.048^{+0.014}_{-0.011}$  pulsars  $\text{yr}^{-1}$  galaxy $^{-1}$ . The quoted errors refer to 95 per cent confidence limits corresponding to fluctuations arising from sampling, but make no allowance for other systematic and random errors which could be substantial. The birthrate estimated here is consistent with the supernova rate. We further conclude that a large majority of pulsars make their first appearance at periods greater than 0.5 s. This ‘injection’, which runs counter to present thinking, is probably connected with the physics of pulsar radio emission. Using a variant of our theory, where we compute the current as a function of pulsar ‘age’ ( $\frac{1}{2}P/\dot{P}$ ), we find support for the dipole braking model of pulsar evolution upto  $6 \times 10^6$  yr of age. We estimate the mean pulsar braking index to be  $3.7^{+0.8}_{-0.8}$ .

*Key words:* pulsar statistics—birthrate—injection

### 1. Introduction

Neutron stars are widely believed to be born in supernova explosions (Baade and Zwicky 1934). The matter in the envelope of the star forms the expanding supernova remnant (SNR) while the core of the progenitor star is compressed into the

highly magnetised and rapidly rotating neutron star which, is believed to manifest itself as a pulsar (Gold 1968). If the above scenario is true, one expects to find a strong association between pulsars on the one hand and Supernovae and SNRs on the other. However, observations have failed to bring this out. On the contrary, there seem to be two important discrepancies:

(a) The birthrates of pulsars and Supernovae in the galaxy are apparently in disagreement. Pulsars are believed to be born once every six to eight years (Taylor and Manchester 1977; Phinney and Blandford 1981). On the other hand, estimates of the birthrate of Supernovae, while varying over a wide range of values (Ilovaisky and Lequeux 1972; Tammann 1974; Clark and Caswell 1976), seem to be converging to one supernova every thirty years (Clark and Stephenson 1977; Srinivasan and Dwarakanath 1981).

(b) Among the 300 or more pulsars and 120 SNRs known, positional associations have been reliably established only in two cases (the Crab and Vela pulsars).

In this paper, the main thrust of our calculations is towards obtaining a more reliable pulsar birthrate. Usually, the birthrate of pulsars is computed by the simple argument that, in steady state conditions, the total number of pulsars  $\mathcal{N}$  in our galaxy should be equal to the birthrate  $B$  multiplied by the mean lifetime of pulsars  $\tau_m$ .  $\mathcal{N}$  is obtained by using the inferred space density of potentially observable pulsars in our galaxy, and multiplying it by a 'beaming-factor'  $K$  which accounts for those pulsars which are not beamed towards the earth. It is believed (Taylor and Manchester 1977) that  $\mathcal{N} \simeq 5 \times 10^5$  pulsars. By assuming the dipole model for pulsar braking (Ostriker and Gunn 1969),  $\tau_m$  can be estimated through the relation  $\tau = \frac{1}{2} P/\dot{P}$  where  $\tau$  is the present age of a pulsar,  $P$  is its period and  $\dot{P}$  is its (dimensionless) period derivative. Alternatively,  $\tau_m$  can also be estimated by dividing the mean height  $\langle z \rangle$  of pulsars above the galactic plane by their mean  $z$ -velocity  $\langle V_z \rangle$  ( $\langle V_z \rangle$  can be obtained indirectly from the proper motions which have been measured for a few pulsars). This 'kinematic' age has the advantage of being independent of errors in pulsar distances. By using a combination of both values of  $\tau_m$ , Taylor and Manchester (1977) computed a birthrate of one pulsar every six years in our galaxy.

In this paper, we have adopted an entirely different approach to the birthrate calculation. We use the concept of pulsar current in the  $P$ - $\dot{P}$  diagram which has been recently introduced by Phinney and Blandford (1981) and Narayan and Vivekanand (1981). We show that the birthrate can be related to the component of current  $J_p$  parallel to the  $P$  axis.  $J_p$  can be estimated from pulsar data *independently of any model of pulsar evolution*. This is a powerful advantage in our calculations since, as mentioned above, previous attempts usually require postulating the dipole model for pulsar braking. The second new feature in our analysis is that we have treated luminosity selection effects in detail. All earlier calculations assumed that selection effects could be handled with a single scale factor from the observed pulsars to the total population in the galaxy. However, it is known (Lyne, Ritchings and Smith 1975) that the luminosities  $L$  of pulsars are correlated with  $P$  and  $\dot{P}$  (hence  $\tau$  also). Consequently, the necessary scale factor differs from one pulsar to the other (Taylor 1981, personal communication). We have carried out this more detailed analysis and find that it makes a significant difference to the answers. We now obtain a mean pulsar birthrate of one pulsar every 21 years which is in comfortable agreement with current estimates of supernova explosion rates.

The paper is divided into two parts (Sections 2 and 3). In Section 2, our analysis is model free and we make very few approximations. The numbers we obtain from these calculations are therefore unbiased. Unfortunately, in the process, we lose in Statistical significance (as anticipated by Phinney and Blandford 1981) and the expected errors on the estimated quantities are very large. A preliminary version of these results was recently published (Narayan and Vivekanand 1981).

Section 3 deals with an ‘improved’ analysis whose main attempt is to reduce the statistical errors. This we have achieved by modelling the dependence of radio luminosity upon  $P$  and  $\dot{P}$  by the following functional form (first used by Lyne, Ritchings and Smith 1975)

$$L' (P, \dot{P}) \propto P^\alpha \dot{P}^\beta \quad (1)$$

where  $L'$  is the ‘mean’ luminosity of pulsars of a given  $P$  and  $\dot{P}$ . By making certain further approximations, which are discussed in Section 3.2, we have computed the scaling factor as a function of  $P$  and  $\dot{P}$  alone. Using a fairly stringent statistical test, we have verified that equation (1) and the approximations made are a fair and unbiased representation of the data. Furthermore, the pulsar birthrate we compute with the new scales is statistically consistent with the result in Section 2, thus increasing our confidence in the new results. As anticipated, there is a significant improvement in the confidence limits of our results, the error bars being reduced by more than a factor of three.

The results of Section 3 are sufficiently accurate to enable us to investigate in coarse detail the variation of  $J_p$  as a function of  $P$ . Surprisingly, we find that  $J_p$  is quite low at small values of  $P$  and picks up significantly at  $P > 0.5$  s. The startling implication of this is that a number of pulsars are ‘born’ in the  $P$ – $\dot{P}$  diagram with fairly large periods. This is totally contrary to the current belief that most neutron stars, and therefore pulsars, are born with periods of the order of a few milliseconds. We therefore conclude that although neutron stars may be born with very short periods (which seems to be suggested by angular momentum considerations), many of them probably turn on as pulsars only somewhat later in their life. Apart from explaining the ‘injection’ of pulsars at higher periods, this suggestion would also naturally account for the lack of many pulsar-SNR associations, which is the second discrepancy mentioned earlier. Of course, we also need to assume that neutron stars cool quickly after birth to explain the lack of X-ray emission from the (hot) surface.

Lastly, we have computed an average value for the ‘braking-index’  $n$ . By comparing  $J_p$  with the current  $J_\tau$  parallel to  $\tau$ , we estimate the braking index to be  $n \simeq 3.7_{-0.8}^{+0.8}$ . This result, which is not inconsistent with the dipole model for pulsar braking ( $n = 3$ ), is important because all earlier studies on pulsar evolution have neglected selection effects as well as pulsar injection and could therefore be seriously in error.

## 2. Model-free approach

### 2.1 Introduction

In this section we present the basic theory of pulsar current  $J_p$  parallel to the  $P$ -axis and its connection with pulsar birthrate. We introduce the scale factor  $S(L)$ , which

gives the ratio of all potentially observable pulsars of luminosity  $L$  in the galaxy to those observed, and describe how it is computed. We apply the theory to the  $P$ ,  $\dot{P}$  and  $L$  data of 210 pulsars (Although more than 300 pulsars have been detected so far, we have ‘pruned’ the data to 210 pulsars for reasons that are given later). Using the theory, we estimate the number of pulsars in our galaxy and also make a model-independent estimation of pulsar birthrate. Finally, we calculate the current  $J_\tau$  parallel to  $\tau$  and find that the dipole model for pulsar braking is a reasonable description of ‘young’ pulsars.

### 2.2 Theory of Pulsar Current

We make the following two postulates:

(a) The distribution of pulsars in the Galaxy is in a steady state. This is reasonable since the lifetimes of pulsars, believed to be a few million years, are much smaller than the lifetime of our galaxy.

(b) The period of a pulsar always increases with age. In support of this is the fact that every observed  $\dot{P}$  is positive.

Let  $\rho(P, \dot{P}, L) dP d\dot{P} dL$  be the number of pulsars in our galaxy in the period range  $P$  to  $P + dP$ , period derivative range  $\dot{P}$  to  $\dot{P} + d\dot{P}$ , and radio luminosity range  $L$  to  $L + dL$ . Since  $\dot{P}$  is the component of pulsar ‘velocity’ parallel to the  $P$ -axis, the ‘current’ of pulsars (number per unit time) at any  $P$  moving from lower values of  $P$  to higher values is evidently given by

$$J_P(P) = \iint \rho(P, \dot{P}, L) \dot{P} d\dot{P} dL \text{ pulsars s}^{-1} \text{ galaxy}^{-1}. \tag{2}$$

It turns out that the statistics are too poor for us to compute the function  $J_P$  with any reliability from the available data. Hence we consider an average of  $J_P$  over a range of period from  $P_{\min}$  to  $P_{\max}$

$$\bar{J}_P(P_{\min}, P_{\max}) = \frac{1}{(P_{\max} - P_{\min})} \int_{P_{\min}}^{P_{\max}} J_P(P) dP. \tag{3}$$

Fig. 1 illustrates the relation between  $J_P$  and  $B$ , the birthrate of pulsars. Since all  $\dot{P}$  are positive, the continuity equation implies that  $J_P(P)$  is identically equal to the total birthrate of pulsars in the period range 0 to  $P$ , minus the death rate in the same

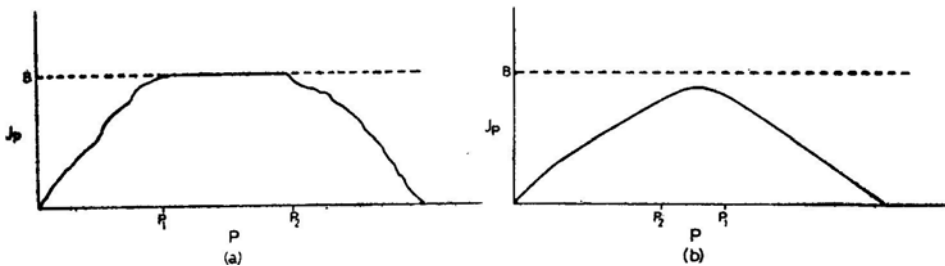


Figure 1. Qualitative plot of pulsar current  $J_P$  against period  $P$ .  $B$  is the total birthrate of pulsars. All births occur for  $0 < P < P_1$  while all deaths occur for  $P > P_2$ . (a)  $P_2 > P_1$ ; (b)  $P_2 < P_1$ .

range. Let all births occur between 0 and  $P_1$  and all deaths occur beyond  $P_2$ . If, as in Fig. 1(a),  $P_2 > P_1$ , then there is a plateau in  $J_p$  between  $P_1$  and  $P_2$  where the function is equal to the total birthrate  $B$ . However, if there is an overlap of births and deaths as in Fig. 1 (b) (*i.e.*  $P_2 < P_1$ ), then  $J_p$  is less than  $B$  at all  $P$ . By the above arguments, it is clear that  $\bar{J}_p (P_{\min}, P_{\max})$  defined in equation (3) is always a lower bound on  $B$  whatever  $P_{\min}$  and  $P_{\max}$  we may choose. In practice, we closely examine the noisy  $J_p$  calculated from experimental data and compute  $\bar{J}_p$  for values of  $P_{\min}$  and  $P_{\max}$  selected at the two edges of the apparent plateau. It is then reasonable to expect that the value of  $\bar{J}_p$  so obtained is a close estimate of  $B$  itself and not just a lower bound.

The total pulsar density  $\rho(P, \dot{P}, L)$  is not directly available. It is related to the observed density function  $\rho_0(P, \dot{P}, L)$  by two factors:

(a) There is a ‘beaming-factor’  $K$  which arises because many pulsars may not be beamed towards us.  $K$  is generally assumed to be 5 (Taylor and Manchester 1977).

(b) There is a scale factor  $S(L)$  which arises because pulsars of a given  $L$  can be detected only upto a certain maximum distance by the instruments currently available.  $S(L)$  also allows for those parts of the sky which have not been searched by the various surveys. We discuss  $S(L)$  in further detail in the next section.

Therefore,

$$\rho(P, \dot{P}, L) = K S(L) \rho_0(P, \dot{P}, L). \tag{4}$$

The observed density function  $\rho_0(P, \dot{P}, L)$  is not known as a continuous function. Instead we have  $P, \dot{P}$  and  $L$  values for  $N$  pulsars. We therefore approximate equation (4) by the following expression

$$\rho(P, \dot{P}, L) \simeq \sum_{i=1}^N K S(L_i) \delta(P - P_i) \delta(\dot{P} - \dot{P}_i) \delta(L - L_i) \tag{5}$$

where  $\delta(x)$  is the Dirac delta function at  $x = 0$ . We may point out that  $\bar{J}_p$  is evaluated as an integral over  $P, \dot{P}$  and  $L$  and therefore the  $\delta$ -functions in equation (5) are always integrated out in the quantities of interest to us. Substituting equation (5) in equation (3), we obtain an estimate of  $\bar{J}_p$  in the form

$$\bar{J}_{P, \text{est}}(P_{\min}, P_{\max}) = \frac{K}{(P_{\max} - P_{\min})} \sum_{i=1}^N S(L_i) \dot{P}_i, \quad P_{\min} \leq P_i \leq P_{\max}. \tag{6}$$

In Appendix A, we have shown that the variance of this estimator is

$$\sigma_J^2 = \frac{K^2}{(P_{\max} - P_{\min})^2} \sum_{i=1}^N S^2(L_i) \dot{P}_i^2, \quad P_{\min} \leq P_i \leq P_{\max}. \tag{7}$$

Equation (7) allows for errors arising from fluctuations in the observed sample but does not take into account possible errors in  $K$  and  $S(L_i)$ .

As mentioned before,  $J_{P, \text{est}}$  would be an unbiased estimator of the birthrate  $B$  if  $P_{\text{min}}$  and  $P_{\text{max}}$  correspond to the true plateau region of  $J_P$  and if the birth and death domains are non-overlapping as in Fig. 1(a). If not,  $\bar{J}_{P, \text{est}}$  is, in any case, an estimator of a rigorous lower bound on  $B$ .

Before closing this section, we briefly discuss the convergence of the integral in equation (2). Phinney and Blandford (1981) claim (i) that the observed distribution of pulsars is free of selection effects (*i.e.* in our notation,  $\rho(P, \dot{P}, L) \equiv K \langle S \rangle \rho_0(P, \dot{P}, L)$  where  $\langle S \rangle$  is a constant scale for all pulsars), (ii) that at large  $\dot{P}$ ,  $\rho_0(P, \dot{P}) \propto \dot{P}^{-1/2}$ , (iii) that therefore the integral in equation (2) is divergent. On these grounds they expect 'kinematic approaches' such as ours to be 'doomed to failure' and have instead attempted a 'dynamical approach'. We, however, find a systematic variation of  $L$  over the  $P$ - $\dot{P}$  plane (see Section 3.2). Therefore our scale factors  $S(L)$  are a necessary and important input for the evaluation of the integral in equation (2). Very roughly,  $S(L)$  is seen to vary as  $\dot{P}^{-1/2}$ . While this anticorrelation of  $S(L)$  with  $\dot{P}$  does not remove the apparent divergence noted by Phinney and Blandford (1981), it certainly improves matters. Moreover, we show in Section 3.4 that there is a cut-off value of  $\dot{P}$  above which pulsars apparently do not function. Such a cut-off will obviously cure all divergence problems. Finally, in the event that there really is a long tail in the distribution of pulsars at high values of  $\dot{P}$ , we are left with the implication that there are many unseen pulsars in the top region of the  $P$ - $\dot{P}$  diagram. If so, all forms of analysis including the dynamical approach are bound to be incomplete.

### 2.3 Scale Factors

We have computed the scale factors,  $S(L)$ , using the parameters of the three major pulsar surveys *viz.* the Jodrell Bank survey (Davies, Lyne and Seiradakis 1972, 1973), the Arecibo survey (Hulse and Taylor 1974, 1975) and the II Molonglo survey (Manchester *et al.* 1978). We used the following equation for  $S(L)$

$$S(L) = \frac{\int \int \int \rho_{R_g}(R_g) \rho_z(z) R_g dR_g d\theta dz}{\int \int \int \rho_{R_g}(R_g) \rho_z(z) \eta(L, R_g, \theta, z) R_g dR_g d\theta dz} \quad (8)$$

where  $\rho_{R_g}$  describes the variation of pulsar density with galactocentric radius  $R_g$  and  $\rho_z$  describes the density as a function of height  $z$  above the galactic plane,  $\theta$  is the polar angle defined with respect to the galactic centre. The parameter  $\eta(L, R_g, \theta, z)$  is set to the value 1 if a pulsar of luminosity  $L$  at coordinates  $R_g, \theta, z$  can be detected by any of the three surveys. Otherwise, it is set to zero. Therefore, the denominator of equation (8) is proportional to the number of pulsars of radio luminosity  $L$  which can be detected by the three reference surveys while the numerator is proportional to all potentially observable pulsars in the galaxy with luminosity  $L$ . In computing  $S(L)$  through equation (8), we have adopted an exponential form for  $\rho_z$  with a scale height of 350 pc (Manchester 1979). For  $\rho_{R_g}$ , we have fitted the experimental histo

gram of number of pulsars against  $R_g$  given by Manchester (1979) to obtain the following gaussian form

$$\rho_{R_g}(R_g) \propto \exp [-(R_g/10.9)^2], \quad (9)$$

where  $R_g$  is measured in kpc. It is interesting that the scale length of 10.9 kpc is close to the radial distance of the sun from the galactic centre. This illustrates the well-known fact that the density of pulsars falls off rapidly with galactocentric radius in the solar neighbourhood. The function (9) is probably incorrect in the range  $0 \leq R_g \leq 4$  kpc where observations seem to suggest a deficit of pulsars. However, this region is only about 10 per cent of the volume of the galaxy and can cause a systematic error of at most 20 per cent in our calculations.

$S(L)$  was calculated at a number of selected values of  $L$  using a Monte Carlo method to evaluate the integrals in equation (8). The luminosities of the observed pulsars were calculated from their radio fluxes and estimated distances. Following the convention of Taylor and Manchester (1977), we have evaluated  $L$  in units of mJy kpc<sup>2</sup>. Distances were calculated from the observed dispersion measures, assuming the interstellar electron density  $n_e$  in the plane of the galaxy to be 0.03 cm<sup>-3</sup> and taking a scale height of 1 kpc for decay of  $n_e$  in the  $z$  direction (Taylor and Manchester 1977). We have corrected for intervening H II regions using a modification of the Prentice and ter Haar (1969) correction, which is discussed in Appendix B. For some pulsars, independent estimates of distance are available (Manchester and Taylor 1977), and these have been adopted in preference to the distances derived from the dispersion measure.

Out of the total of 302 pulsars detected, we have selected a 'pruned' list of 210 pulsars so as to obtain a uniform sample of pulsars consistent with the scale factors  $S(L)$ . The pruning was done on the basis of two criteria:

(a) The pruned list should contain only those pulsars which were detected by the three reference surveys. This precaution is necessary since we have computed  $S(L)$  using only these three surveys.

(b) In computing  $S(L)$  we have used the published parameters (such as sensitivity, sky coverage *etc.*) of the three surveys. Since the data base should also be consistent with these parameters, we have omitted those pulsars whose radio fluxes were below the quoted minimum flux detection levels of the surveys. At this stage, it would have been ideal to take into account the intrinsic intensity variations displayed by many pulsars. This would further affect the observability of pulsars by the three surveys, thereby affecting the computation of  $S(L)$ . However, this would require detailed information such as the phase of the intensity variation of each pulsar at the time of search. For lack of information, we have chosen to ignore this complication.

After pruning, we were left with 210 pulsars, of which we knew the  $\dot{P}$  values of 185 pulsars and  $L$  values of 207 pulsars. Individual scale factors  $S(L)$  were then computed for all the pulsars with known  $L$  values by suitably interpolating in the table of  $S(L)$  values which we had calculated earlier.

#### 2.4 Number of Pulsars in the Galaxy

The total number of pulsars in the galaxy is given by

$$\mathcal{N} = \iiint \rho(P, \dot{P}, L) dP d\dot{P} dL \quad (10)$$

which can be written in terms of the observed  $\rho_0$  as

$$\mathcal{N} = K \iiint S(L) \rho_0(P, \dot{P}, L) dP d\dot{P} dL. \quad (11)$$

Using equation (5) for  $\rho_0$ , we obtain the following estimate for  $\mathcal{N}$ .

$$\mathcal{N}_{\text{est}} = K \sum_{i=1}^N S(L_i). \quad (12)$$

The standard deviation  $\sigma_{\mathcal{N}}$  of  $\mathcal{N}_{\text{est}}$  can be shown to be given by (Appendix A)

$$\sigma_{\mathcal{N}}^2 = K^2 \sum_{i=1}^N S^2(L_i). \quad (13)$$

Using the data on 210 pulsars, we obtain  $\mathcal{N}_{\text{est}}$  to be  $6.05 (\pm 1.88) \times 10^5$  pulsars. Now, the error limits specified by  $\pm \sigma_{\mathcal{N}}$ ,  $\pm 2\sigma_{\mathcal{N}}$ , etc., have well defined meanings only if the distribution of  $\mathcal{N}_{\text{est}}$  is gaussian. This is not so in the present case because  $S(L)$  is spread over five orders of magnitude. The bulk of  $\mathcal{N}_{\text{est}}$  in equation (12) is actually contributed by only a few of the highest values of  $S(L)$ . We can therefore expect the distribution of  $\mathcal{N}_{\text{est}}$  to be highly asymmetric and non gaussian. Consequently, a more meaningful concept in the present case is the confidence limit. We have derived the following upper and lower bounds on  $\mathcal{N}_{\text{est}}$  at a 95 per cent confidence level (the method of calculating these confidence limits is briefly given in Appendix C).

$$\mathcal{N}_{\text{est}} | 95 \text{ per cent, lower} = 3.19 \times 10^5 \text{ pulsars}, \quad (14)$$

$$\mathcal{N}_{\text{est}} | 95 \text{ per cent, upper} = 9.37 \times 10^5 \text{ pulsars}. \quad (15)$$

The limits in equations (14) and (15) are formal estimates of fluctuations arising from the Poissonian nature of the observed sample of pulsars. In addition, there could be significant errors in  $S(L_i)$ , arising from uncertainties in the distances of pulsars ( $n_e$  is not known reliably) and in  $K$ . It should be remembered that these unestimated errors could be comparable to if not larger than the formal errors quoted here and in all subsequent sections of the paper. Arnett and Lerche (1981) have, in fact, concluded that the uncertainties in  $K$  and  $n_e$  are so large and certain other details, not relevant in our analysis, are so poorly understood that any statistical analysis of pulsar data is meaningless. We take a more optimistic view.

Our results for  $\mathcal{N}$  are in good agreement with the currently accepted value (Taylor and Manchester 1977) of  $\mathcal{N} \simeq 5 \times 10^5$ . This is an independent check on our analysis and, in particular, on our values of  $S(L)$ .

### 2.5 Pulsar Birthrate

We estimate the birthrate by the 'plateau-value' of  $\bar{J}_{P, \text{est}}$  ( $P_{\text{min}}, P_{\text{max}}$ ) as described in Section 2.2. Fig. 2 shows the values of  $\bar{J}_{P, \text{est}}$  in various 0.5 s bins of period. The



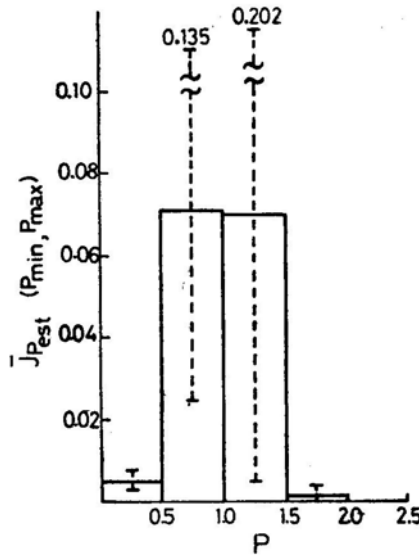


**Figure 2.** Plot of estimated mean pulsar current  $\bar{J}_{P, \text{est}}$  against period  $P$ . Error limits are specified at a 95 per cent confidence level.  $J_P$  has been averaged over period intervals of 0.5 s. However, the qualitative nature of the histogram remains unchanged under finer binning in period. Scale values  $S(L)$  (derived from observed luminosities) have been used.

bin size was selected so as to have the best combination of good resolution in period and good error estimates. It would appear from Fig. 2 that a plateau exists from  $P_{\text{min}} = 0.5$  s to  $P_{\text{max}} = 1.5$  s. We thus estimate the birthrate of pulsars to be

$$B \simeq \bar{J}_{P, \text{est}}(0.5, 1.5) = 0.07_{-0.05}^{+0.07} \text{ pulsars yr}^{-1} \text{ galaxy}^{-1} \quad (16)$$

or one pulsar born every  $14_{-7}^{+33}$  years, where the error limits correspond to the lower and upper bounds at 95 per cent confidence. The above result is slightly different from, but consistent with, the value we had published earlier (Narayan and Vivekanand 1981). The difference arises because  $P_{\text{min}}$  was earlier taken to be 0s. Keeping in mind that the error bounds refer to the 95 per cent confidence limits, and that the present analysis is approximation free and model independent, we consider the results satisfactory. However, we obtain tighter estimates in Section 3

### 2.6 Birthrate on the Basis of a Dipole Model of Braking

We briefly discuss a modification of our theory which permits us to estimate the birthrate assuming the dipole braking model of pulsar evolution.

Let  $\rho'_0(\tau, L) d\tau dL$  be the observed density of pulsars with radio luminosity between  $L$  and  $L + dL$  and age ( $\tau = \frac{1}{2}P/\dot{P}$ ) between  $\tau$  and  $\tau + d\tau$ . If  $\tau$  is true age, then the 'velocity' of pulsars along the  $\tau$  axis is  $\dot{\tau} = 1$ . Therefore, the current  $J_\tau$  of pulsars at an age  $\tau$  parallel to the  $\tau$ -axis is given by

$$J_\tau(\tau) = \int KS(L) \rho'_0(\tau, L) dL. \quad (17)$$

As before  $J_\tau$  is equal to the birthrate of pulsars in the age range from 0 to  $\tau$  minus

the deathrate in the same range. Once again, for better statistics, we average  $J_\tau$  from  $\tau_{\min}$  to  $\tau_{\max}$ .

$$\bar{J}_\tau(\tau_{\min}, \tau_{\max}) = \frac{K}{(\tau_{\max} - \tau_{\min})} \int_{\tau_{\min}}^{\tau_{\max}} J_\tau(\tau) d\tau. \quad (18)$$

An estimator of this quantity is

$$\bar{J}_{\tau, \text{est}}(\tau_{\min}, \tau_{\max}) = \frac{K}{(\tau_{\max} - \tau_{\min})} \sum_{i=1}^N S(L_i), \quad \tau_{\min} \leq \tau \leq \tau_{\max}. \quad (19)$$

Equation (19) is similar to the birthrate formula of Davies, Lyne and Seiradakis (1977) except that we use individual scales for the pulsars and also introduce finite  $\tau_{\min}$  which is 0 in their analysis.

In Fig. 3 we have shown  $\bar{J}_{\tau, \text{est}}$  in bins of  $3 \times 10^6$  years. Since the error bars on  $\bar{J}_{\tau, \text{est}}$  are rather large, it is difficult to locate the plateau region with any confidence. If we take the plateau to extend from 0 to 6 million years, we obtain a birthrate of  $0.04_{-0.02}^{+0.04}$  pulsar  $\text{yr}^{-1}$  galaxy $^{-1}$ , or one pulsar every  $25_{-14}^{+45}$  years. This result is consistent with our earlier result (Section 2.5), suggesting that young pulsars upto 6 million years of age may be evolving according to the dipole braking law. Fig. 3 shows a

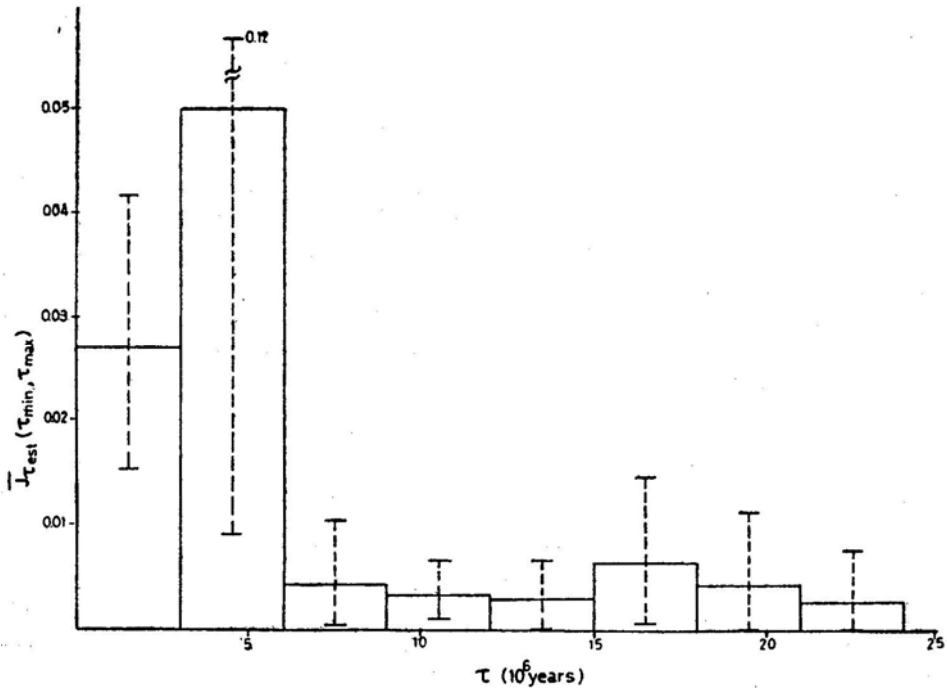


**Figure 3.** Plot of estimated mean pulsar current  $\bar{J}_{\tau, \text{est}}$  against apparent pulsar age  $\tau = \frac{1}{2}P/\dot{P}$ .  $J_\tau$  has been averaged over age intervals of 3 million years. Error limits are specified at a 95 per cent confidence level.  $J_\tau$  definitely drops from the first to the third bin, although  $J_\tau$  in the second bin is not determined clearly. There is no detectable change in  $J_\tau$  for bins of higher apparent ages. Scale values  $S(L)$  have been used.

significant drop in the value of  $\bar{J}_{\tau, \text{est}}$  after 6 million years. This suggests that, beyond 6 million years, either pulsars could be dying or the relation,  $\text{age} \equiv \frac{1}{2}P/\dot{P}$ , may no longer be valid (say, due to magnetic field decay).

### 2.7 Importance of Radio Luminosity Selection Effects

Is the radio luminosity selection effect important for the computation of the birthrate? We can answer this by comparing the birthrate of Section 2.5 with a second calculation where all pulsars are weighted by a *single average* scale  $\langle S(L) \rangle$ . Equation (6) would then become

$$\bar{J}_{P, \text{est}}(P_{\min}, P_{\max}) = \frac{K \langle S(L) \rangle}{(P_{\max} - P_{\min})} \sum_{i=1}^N \dot{P}_i, \quad P_{\min} \leq P_i \leq P_{\max}. \quad (20)$$

We have made a thorough statistical comparison of the currents calculated by equations (6) and (20) on the basis of which we can state with greater than 80 per cent confidence that the two quantities are not the same. The analysis of Section 3 reinforces this statement with much greater confidence. We are therefore quite certain that radio luminosity selection effects are vitally important and should not be neglected. This calls for a re-examination of all earlier analyses of pulsar data.

## 3. Luminosity model approach

### 3.1 Introduction

In Section 2, we computed the pulsar birthrate from  $\bar{J}_{P, \text{est}}$  (equation 6) using the scale factors  $S(L)$  derived from the observed radio luminosities. Since the values of  $L$  are spread over four to five orders of magnitude,  $S(L)$  is spread over a similar range. This results in a high variance for  $\bar{J}_{P, \text{est}}$ . In this section we have used new scales whose variance is smaller. This we have achieved by modelling the dependence of radio luminosity upon  $P$  and  $\dot{P}$  as specified in equation (1). We have thus derived 'mean' radio luminosities  $L'$  which have a 'smooth' dependence upon  $P$  and  $\dot{P}$ , in contrast to the old  $L$  values. Furthermore, we have allowed for the fact that, at a given  $P$  and  $\dot{P}$ , there is a *distribution* of  $L$  around  $L'$ . Using this distribution we calculate a mean scale value  $S'(P, \dot{P})$  at any  $P$  and  $\dot{P}$ . The scatter in these new scales is reduced from five to three orders of magnitude. Consequently, there are much smaller statistical errors in the new estimates for the birthrate and other quantities. On the other hand, the assumed luminosity model could lead to systematic errors.

From a detailed analysis of the pulsar current  $J_P$ , we reach the important conclusion that a significant fraction of pulsars are 'born' in the period range 0.5 s to 1.0 s. This result, which we describe as 'injection', could have strong implications for theories concerning the birth of pulsars, their radiation mechanism and their evolution in the  $P$ - $\dot{P}$  diagram. We have approximately identified the area of the  $P$ - $\dot{P}$  diagram where injection is the strongest, and have suggested a possible explanation.

Finally, we have derived a mean value for the braking index of pulsars. We find it not inconsistent with the values in current use.

### 3.2 Model for Luminosity Correlations

We have fitted a least squares plane to the data of  $\log L$  against  $\log P$  and  $\log \dot{P}$  available for 242\* pulsars to obtain the 'mean' luminosity  $L'$  (see equation 1) in the form

$$\dot{L}'(P, \dot{P}) \propto P^{-0.86(\pm 0.2)} \dot{P}^{0.38(\pm 0.08)} \quad (21)$$

where the numbers in brackets represent  $1\sigma$  errors, computed in the usual way for correlated parameters. Lyne, Ritchings and Smith (1975) did a similar exercise and obtained  $L' \propto P^{-1.8} \dot{P}^{0.88}$ . However, they did not fit a least-squares plane but instead arrived at their result by maximizing a correlation coefficient between  $L$  and a known function of  $P$  and  $\dot{P}$ . This may explain the discrepancy between their results for the exponents and ours. To check this we fitted a least squares plane to the data of 84 pulsars used by them and obtained  $L' \propto P^{-0.79(\pm 0.30)} \dot{P}^{0.36(\pm 0.11)}$  which is consistent with our result in equation (21).

We now make the crucial approximation that the observed density distribution of pulsars  $\rho_0(P, \dot{P}, L)$  can be separated into the product of two functions in the form

$$\rho_0(P, \dot{P}, L) = \rho_1(P, \dot{P}) \rho_2(\log L - \log L'(P, \dot{P})) \quad (22)$$

where  $\rho_1$  is the density of pulsars in the  $P-\dot{P}$  plane,  $\rho_2$  is normalized to 1 and  $L'(P, \dot{P})$  is defined in (21). We are thus assuming that the distribution of  $\log L$  is the same at all points in the  $P-\dot{P}$  plane except for the shift given by  $\log L'(P, \dot{P})$ . We have made the following sensitive statistical test of this hypothesis. We divided the  $P-\dot{P}$  plane into four quadrants, each containing approximately the same number of pulsars. In each quadrant we separately tabulated the values of  $[\log L - \log L'(P, \dot{P})]$  of the observed pulsars. Taking five bins in this variable, we carried out a  $\chi^2$ -test to verify that the distributions in the four quadrants are the same. We obtained a  $\chi^2$  value of 13.6 while the number of degrees of freedom of the test is 12. There is thus very good statistical evidence for supporting the hypothesis in equation (22).

Equation (22) can be written in the equivalent form

$$\rho_0(P, \dot{P}, L) = \rho_1(P, \dot{P}) \rho'_2(L/L'(P, \dot{P})) \quad (23)$$

where again  $\rho'_2$  is normalized to 1. The mean scale factor  $S'(P, \dot{P})$  at a given  $(P, \dot{P})$  is then obviously given by

$$S'(P, \dot{P}) = \int_0^\infty \rho'_2(L/L'(P, \dot{P})) S(L) dL \quad (24)$$

\*To date,  $\dot{P}$  values have been measured for 256 pulsars. But  $L$  values are not available for 14 of them.

where  $S(L)$  is the old scale factor defined in Section 2.2.  $S'(P, \dot{P})$  can be approximately calculated in terms of the data on the 242 pulsars (for which  $P$ ,  $\dot{P}$  and  $L$  are available) by means of the expression

$$S'(P, \dot{P}) = \frac{1}{242} \sum_{j=1}^{242} S(\xi_j(P, \dot{P})) \quad (25)$$

where

$$\xi_j(P, \dot{P}) = L'(P, \dot{P}) L_j / L'(P_j, \dot{P}_j). \quad (26)$$

We have computed  $S'(P_i, \dot{P}_i)$  for each of the 185 pulsars in the pruned list (of 210 pulsars) for which  $\dot{P}_i$  are available and these have been used in the calculations discussed in the rest of Section 3.

To summarize, in this section we calculate the scale factor of a pulsar, not in terms of its *observed luminosity* but in terms of the *expected distribution of luminosity* at the particular values of  $P$  and  $\dot{P}$ . At the heart of this approximation is the basic assumption (equations 21 and 22) that the luminosity distribution is the same at all  $P$  and  $\dot{P}$  except for the scaling by  $L'(P, \dot{P})$ . We are convinced of the validity of this assumption on the basis of the statistical test that we have conducted. With the new scales  $S'(P_i, \dot{P}_i)$  we are able to make a much more thorough analysis of the data than was possible in Section 2 with the old scales  $S(L_i)$ .

### 3.3 Pulsar Birthrate

Using the new scales, equation (6) becomes

$$\bar{J}'_{P, \text{est}}(P_{\min}, P_{\max}) = \frac{K}{(P_{\max} - P_{\min})} \sum_{i=1}^N S'(P_i, \dot{P}_i) \dot{P}_i, \quad P_{\min} \leq P_i \leq P_{\max}. \quad (27)$$

We have plotted  $\bar{J}'_{P, \text{est}}$  in Fig. 4. Comparison with Fig. 2 shows that the new scales have significantly improved the error limits. The plateau appears to extend from  $P = 0.5\text{s}$  to  $P = 1.5\text{s}$ . The mean value of  $\bar{J}'_{P, \text{est}}$  in this range is  $0.048^{+0.014}_{-0.011}$ , giving a birthrate of one pulsar every  $21^{+6}_{-5}$  years in the galaxy. This is consistent with the number derived in Section 2.5, but has much smaller error limits. It now becomes meaningful and interesting to compare our estimated pulsar birthrate with the supernova rate.

Unfortunately, a reliable estimate of the supernova rate is not available. It is obtained both from direct observations of supernova explosions in external galaxies and from a study of historical Supernovae and SNRs in our galaxy. Estimates from studies of external galaxies range right from one explosion in 359 years (Zwicky 1962) to one every 11 years (Tammann 1977). Studies of historical Supernovae in our galaxy have yielded one explosion every 30 years (Katgert and Oort 1967; Clark and Stephenson 1977). Studies of SNRs in our galaxy have given one explosion every 60 years (Poveda and Woltzer 1968; Milne 1970; Downes 1971)

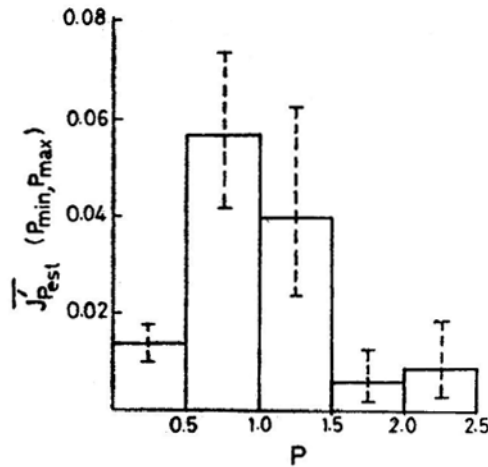


**Figure 4.** Same as Fig. 2, but with improved scale values  $S'(P, \dot{P})$  derived from  $P$  and  $\dot{P}$ .  $J_p$  increases in the second bin, drops only marginally in the third, and drops significantly in the fourth bin, closely following Fig. 1 (a).

However, a recent work (Srinivasan and Dwarakanath 1981) on SNRs has estimated that supernova explosions in the Galaxy occur once every 25 years. If we accept this number, there is no significant discrepancy between the birthrates of pulsars and Supernovae.

The dramatic reduction in the error limits from equation (6) to equation (27) is easily understood. Both  $S(L_i)$  and  $\dot{P}_i$  in (6) vary over many orders of magnitude (almost independently). On the other hand, as a consequence of the luminosity model which we have introduced,  $S'(P_i, \dot{P}_i)$  varies approximately as  $\dot{P}^{-1/2}$  and is therefore anticorrelated with  $\dot{P}$ . Thus the range of values in the summation in equation (27) is several orders of magnitude less than in equation (6), leading to much improved Statistical significance. Another way of stating it is that the effective number of pulsars contributing, to equation (16) [computed by the approximate. expression  $(B/\sigma_B)^2$ ] is only 6 while it is nearly 60 for equation (27)

### 3.4 Injection

We now discuss a very important result of our analysis. We see in Fig. 4 that  $\bar{J}_p$ , est is significantly higher in the second bin, compared to the first. The mean value is four times higher and even the 95 per cent lower limit in bin 2 is higher than the 95 per cent upper limit in bin 1. It is clear that such a situation can arise only if some pulsars make their appearance in bin 2 without 'flowing' through bin 1. In other words, some radio pulsars are apparently being 'born' in the period range of 0.5 to 1.0 s. We have verified that this 'injection' is not sensitive to the particular choice of bin size. It is also not an artifact of the new analysis with  $S'(P, \dot{P})$  since there is compelling evidence for injection even in the rigorous analysis of Section 2 (see also Fig. 1 of our earlier publication, Narayan and Vivekanand; 1981).

In order to understand the details of injection, we have subdivided each bin in Fig. 4 into three further bins in  $\dot{P}$ . The estimated: mean current  $\bar{J}'_p$  in the various bins are shown in Table 1, along with the 95 percent confidence limits in some cases.

**Table 1.** Estimated mean, pulsar, current  $\bar{J}'_{p, \text{est}}$  in various bins of the  $P-\dot{P}$  diagram. The 95 per cent upper and lower limits to the current are also specified in the important bins.  $P$  is in units of seconds, and  $\dot{P}$  in units of seconds per second.

	$0.0 \leq P < 0.5$	$0.5 \leq P < 1.0$	$1.0 \leq P < 1.5$	$1.5 \leq P < 2.0$
$1 \times 10^{-14} \leq \dot{P} < 1 \times 10^{-11}$	$\cdot 0042^{+\cdot 0031}_{-\cdot 0022}$	$\cdot 0275^{+\cdot 0139}_{-\cdot 0117}$	$\cdot 0169^{+\cdot 0176}_{-\cdot 0124}$	$\cdot 0027$
$1 \times 10^{-15} \leq \dot{P} < 1 \times 10^{-14}$	$\cdot 0067^{+\cdot 0016}_{-\cdot 0018}$	$\cdot 0120^{+\cdot 0052}_{-\cdot 0053}$	$\cdot 0133^{+\cdot 0061}_{-\cdot 0057}$	$\cdot 0025$
$1 \times 10^{-19} \leq \dot{P} < 1 \times 10^{-15}$	$\cdot 0013$	$\cdot 0028$	$\cdot 0037$	$\cdot 0018$

There seems to be strong evidence that injection occurs at *high* values of  $\dot{P}$  in the period range 0.5 s to 1.0 s and possibly even in the 1.0 s to 1.5 s range. We have outlined this high injection region by means of the box in Fig. 5.

The injected pulsars are unlikely to be the 'recycled' pulsars formed in massive close binary systems (de Loore, de Greve and de Cuyper 1975), because of the following reasons.

(a) Even if all pulsars are born in massive close binary systems, the recycled pulsars cannot be more than 50 per cent of the total population. A more realistic estimate based on the actual number of such binary systems (van den Heuvel 1977) would be a few per cent. But the 95 per cent lower bound of  $\bar{J}'_{p, \text{est}}$  in bin 2 (Fig. 4) is more than twice the 95 per cent upper bound of  $\bar{J}'_{p, \text{est}}$  in bin 1, indicating that much more than 66 per cent of the pulsars are injected.

(b) There is no compelling reason to expect predominantly high values of  $\dot{P}$  in such pulsars. On the contrary, low values of  $\dot{P}$  are likely to occur if the magnetic field of pulsars decays on a time scale of  $\simeq 5 \times 10^6$  years, which is the estimated time between the two explosions (de Loore, de Greve, de Cuyper 1975). Injection, on the other hand, occurs at high values of  $\dot{P}$  as shown by Table 1.

Having rejected the 'recycled' pulsars, another possibility is that neutron stars may be born with large periods of the order of 0.5 s. However, it is widely believed (see, for example, Manchester and Taylor 1977) that there are some theoretical difficulties in getting stars to shed most of their angular momentum either before, during, or shortly after collapse (into a neutron star). Therefore we may expect neutron stars to be born with periods of the order of tens of milliseconds. There appears to be some observational support for this, in that at least a certain category of pulsars (*i.e.* those which are not injected) are born with small periods, *viz.* the Crab and Vela pulsars\*. Therefore, we may expect the injected pulsars also to start their careers with low periods, say 10 ms. Now, the dipole model of pulsar braking would predict (in the absence of magnetic field decay) that the pulsars in the injection box in Fig. 5 would have had initial  $\dot{P}$  values  $\simeq 5 \times 10^{-12} \text{ s s}^{-1}$  which is an order of magnitude more than the  $\dot{P}$  of the Crab pulsar. It is therefore surprising that we do not see more pulsars with small values of  $P$  and high values of  $\dot{P}$ .

\*Incidentally, since the injected pulsars form the hulk of the pulsar population, the Crab and Vela pulsars are by no means prototypes of young pulsars.

A close examination of Fig. 5 shows that there is apparently an abrupt cut-off of pulsars above a certain value of  $\dot{P}$ . We have made the following statistical test to determine whether the scarcity of pulsars at high values of  $\dot{P}$  is indeed significant. We tentatively placed the cutoff line at  $\log \dot{P} = -12.5$  (Fig. 5). We assumed a dipole braking model without field decay (which is reasonable for this part of the  $P$ - $\dot{P}$  diagram), and a pulsar 'death' line of the form  $\dot{P} P^{-5} = \text{constant}$  (Ritchings, 1976 has shown that at small values of  $\dot{P} P^{-5}$ , pulsars spend increasing lengths of time in the nulled state, apparently as a prelude to death). Assuming the period at birth to be 10 ms, we computed the birthrate of pulsars in various bins of  $\dot{P}$  using the observed sample of pulsars and the scale factors  $S(P, \dot{P})$ . We then evolved the pulsars according to the dipole braking model and computed the number of pulsars we *should have observed* above the cut-off line. This turns out to be 6.6 pulsars. Since some of these might have been missed by the various pulsar surveys due to their having very low periods, we also computed the expected number of pulsars above the cut-off line with  $P > 100$  ms. Our calculations show that we ought to have seen 2.9 pulsars in this region whereas we actually see none. We can therefore state with

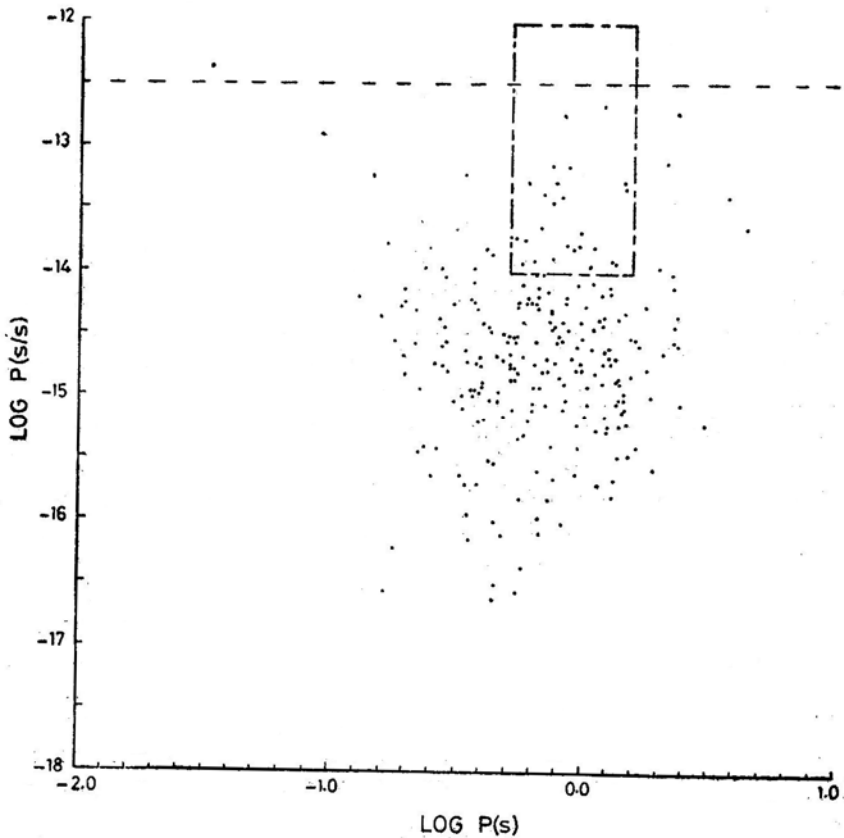


**Figure 5.**  $P$  and  $\dot{P}$  plotted on log-log scale for 256 pulsars. Pulsars appear to be missing above a critical value of  $\dot{P}$ , tentatively represented by the dashed 'cut-off' line. Pulsars are born in the top left part of the diagram (the majority, being born apparently above the cutoff line), and evolve towards the bottom right of the diagram. Most of the pulsar injection occurs in the box at the top of the diagram.



94.5 per cent confidence ( $100 \{1 - \exp(-2.9)\}$ ) that there is a genuine deficit of pulsars above the cut-off line in Fig. 5. We have verified that the above results are not very sensitive to the exact location of either the cut-off line or the death line. However, we cannot reject the possibility that the injection line is actually a more complicated curve than a single horizontal line. For instance, the distribution of points in Fig. 5 might suggest a line with negative slope in the period range from 0 to  $\sim 0.3$  s and a second line with positive slope beyond 0.3 s at the top of the  $P-\dot{P}$  diagram; there could also be an injection line with negative slope at the left of the  $P-\dot{P}$  diagram. Some of these possibilities have been discussed by Radhakrishnan (1981) on the basis of an interesting model.

We would like to offer the following tentative explanation of injection. It is possible that neutron stars do not radiate in the radio region immediately on birth but do so later in their life. We suggest that neutron stars with  $\dot{P}$  greater than the critical value are unable to radiate in the radio. They switch on as pulsars when their  $\dot{P}$  decreases to the appropriate value. Therefore, neutron stars with initial  $\dot{P}$  values above the cut-off line will ‘enter’ the pulsar  $P-\dot{P}$  diagram at higher periods, thereby giving rise to injection. At present, we have no theory or mechanism of pulsar radiation which could explain an upper cut-off line in  $\dot{P}$ . This is currently under investigation.

The above scenario also explains why there are so few pulsar-SNR associations. Our data suggests that pulsars could spend  $\sim 10^4$  year or more above the cut-off line. If SNRs dissolve into the interstellar medium on time scales comparable to the switching-on times of pulsars (there is good evidence for this in the work of Srinivasan and Dwarkanath 1981), there would be very few observable associations between pulsars and SNRs. As mentioned earlier, in this picture we also require that neutron stars should cool rapidly after birth to avoid radiating thermal X-rays.

### 3.5 Braking Index

The braking index  $n$  is defined by the equation

$$\dot{\Omega} \propto -\Omega^n \tag{28}$$

where the angular velocity  $\Omega = 2\pi/P$ . In the dipole braking theory,  $n = 3$ . The age  $\tau$  of a pulsar, assuming the initial period to be 0 s, can be expressed in terms of the braking index as

$$\tau = \frac{1}{(n-1)} \frac{P}{\dot{P}} = \frac{\tau'}{(n-1)} \tag{29}$$

where  $\tau'$  is the characteristic time,  $P/\dot{P}$ . The ‘velocity’ of a pulsar parallel to  $\tau'$  is  $\tau' = (n-1)$ . Hence, the mean pulsar current parallel to  $\tau'$  can be written, as in earlier sections, as

$$\bar{J}_{\tau', \text{est}}(\tau'_{\text{min}}, \tau'_{\text{max}}) = \frac{K}{(\tau'_{\text{max}} - \tau'_{\text{min}})} \sum_{i=1}^N (n_i - 1) S'(P_i, \dot{P}_i), \tau'_{\text{min}} \leq P_i/\dot{P}_i \leq \tau'_{\text{max}}. \tag{30}$$

If we define  $\langle n \rangle$  as the mean braking index of the pulsars in the  $\tau'$  range defined in equation (30), then the equation can be written as

$$\begin{aligned} \bar{J}_{\tau', \text{ est}}(\tau'_{\min}, \tau'_{\max}) &= \frac{K(\langle n \rangle - 1)}{(\tau'_{\max} - \tau'_{\min})} \sum_{i=1}^N S'(P_i, \dot{P}_i) \\ &= (\langle n \rangle - 1) X(\tau'_{\min}, \tau'_{\max}), \quad \tau'_{\min} \leq P_i/\dot{P}_i \leq \tau'_{\max}. \end{aligned} \quad (31)$$

We have plotted  $X(\tau'_{\min}, \tau'_{\max})$  in bins of 2 million years in Fig. 6. The curve appears to be essentially constant (barring the fluctuation in bin 3) up to about  $12 \times 10^6$  yr, and falls thereafter. If we assume the dipole model and take the age as  $\tau'/2$ , then it would appear that up to about  $6 \times 10^6$  yr, the current is constant. Incidentally, in terms of  $\tau'$ , injection occurs below  $10^5$  yr and can therefore be neglected in the discussion here.

Since the histogram in Fig. 6 does not change from  $\tau' = 0$  to  $\tau' = 12 \times 10^6$  yr, this strongly suggests that the mean braking index  $\langle n \rangle$  is essentially constant in this range. Moreover, one can further conclude that there are probably no significant pulsar births or deaths. By an argument similar to that in Section 2.2 one therefore arrives at the interesting result that  $\bar{J}'_{\tau', \text{ est}}(0, 12 \times 10^6 \text{ yr})$  should be comparable to the birthrate  $B$  of pulsars. Since we have an independent estimate of  $B$  in Section 3.3, we can therefore use quotation (31) to obtain an estimate of  $\langle n \rangle$ . We obtain  $\langle n \rangle = 3.7^{+0.8}_{-0.8}$  where the error limits are the 95 per cent confidence limits. It is interesting that our independent estimate of  $\langle n \rangle$ , based only on observational

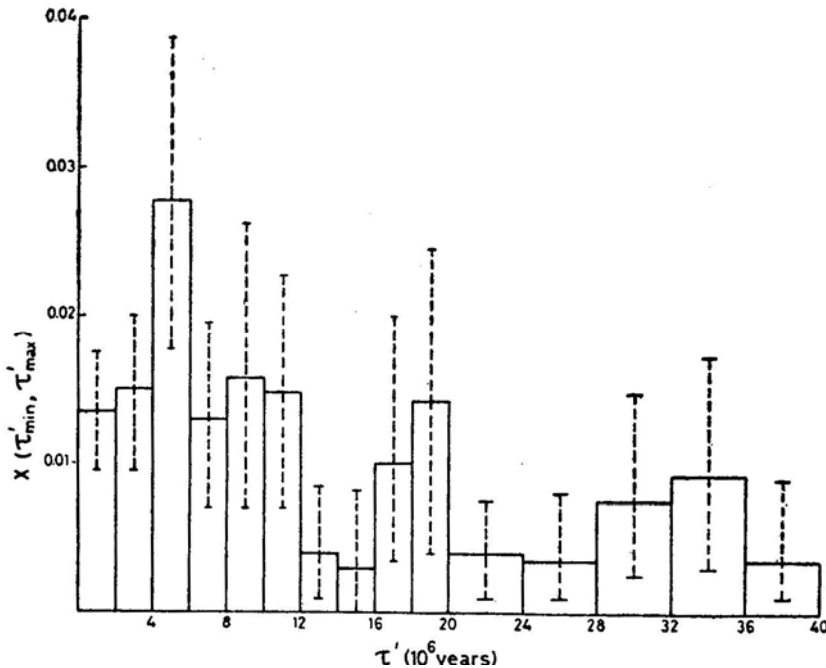


**Figure 6.** Plot of modified pulsar current  $X$  against apparent age  $\tau' = P/\dot{P}$ .  $X$  has been averaged in  $\tau'$  intervals of  $2 \times 10^6$  yr upto  $\tau' = 20 \times 10^6$  yr, and in intervals of  $4 \times 10^6$  yr thereafter. There appears to be no apparent change in the current upto  $12 \times 10^6$  yr.

data, is fairly consistent with, the dipole model value of  $n = 3$ . Incidentally, if we assume the death line of Ritchings (1976), it will be seen that some of the high magnetic field pulsars would die at  $\tau$  values smaller than  $12 \times 10^6$  yr. In that case  $\bar{J}\tau_{\text{est}}(0, 12 \times 10^6 \text{ yr})$  would be smaller than  $B$  and the above value of  $\langle n \rangle$  would be an overestimate. This strengthens the argument in favour of dipole braking in young pulsars (with ages upto  $6 \times 10^6$  yr).

The braking index has been measured independently only for the Crab pulsar (Groth 1975), yielding the value 2.515. We do not consider this to be inconsistent with our  $\langle n \rangle$  because, by our results, the Crab belongs, to a minority class of un-injected pulsars. Further, we have estimated only the *mean* braking, index for the whole pulsar population. We have no information on the individual variations in  $n$  from one pulsar to the other.

#### 4. Conclusions

We may identify the following important sources of error in our calculations.

(a) All our results are based on the observed pulsars. Since the observed sample could differ from the true distribution due to sampling fluctuations, there are statistical uncertainties associated with our numerical results. We have estimated these on a Poissonian assumption and quoted them as 95 per cent confidence limits wherever applicable.

(b) We have assumed the beaming factor  $K$  to have a value 5. However, the true value could be significantly different (*e.g.* Kundt 1981).

(c) We have taken the mean interstellar electron density  $n_e$  to be  $0.03 \text{ electrons cm}^{-3}$ . Since this is used in all distance calculations, it is a highly important input. There could be some uncertainty in the value of  $n_e$  though the value we have adopted is generally accepted as a good estimate over a large portion of the galaxy. Fluctuations in  $n_e$  in different parts of the galaxy could also contribute to the error.

(d) The calculations in Section 3 critically depend on the luminosity model, equations (21) and (22). This could introduce some error in the results. However, since all the major conclusions of Section 3 are consistent with the results of Section 2 where no model is assumed, we believe this error is quite small.

(e) There may be some errors in the computed scaling factors  $S(L_i)$  and also in the manner of pruning the data, arising from possible faulty interpretations of the parameters and selection effects of the three pulsar surveys.

Of the above, errors (d) and (e) are probably not very significant. Errors of the type (a) can be calculated and have been quoted throughout. Errors (b) and (c) have not been estimated though they could be quite large. These errors are present in all earlier analyses, of pulsar data as well. It is also important to note that among our major conclusion listed below, errors (b) and (c) affect only our estimate of pulsar birthrate and have little or no bearing on the rest.

The main conclusions of our study are:

(a) A significant fraction of pulsars are born with initial periods  $> 500$  ms. Therefore the conventional picture of pulsar evolution in the  $P-\dot{P}$  diagram may require significant modifications. The injection of pulsars at high periods should be related to the physics of pulsar radio emission. We suggest that neutron stars probably

switch on as pulsars only when  $\log \dot{P} < -12.5$ . This hypothesis would also explain the lack of SNR—pulsar associations. Our demonstration of injection is based on the rigorous, *model independent* calculations of Section 2 (see Fig. 2), Section 3 serving as a confirmation. Moreover, the result is independent of the particular choice of  $K$  and  $n_e$ .

(b) The birthrate of pulsars is estimated to be  $0.048_{-0.011}^{+0.014}$  (one pulsar every  $21_{-5}^{+6}$  yr), which appears to be consistent with the rate of supernova explosions if (i) every explosion results in a neutron star, and (ii) every neutron star becomes a pulsar sometime in its life. Our estimate is really a lower bound, but we expect it to be close to the actual birthrate because the ‘plateau’ in Fig. 4 shows some resemblance to Fig. 1(a). However, it should be noted that our result depends upon the values chosen for  $K$  and  $n_e$ , neither of which is known with great precision.

(c) The number density of pulsars in the  $P-\dot{P}$  diagram is significantly affected by radio luminosity selection effects which cannot, therefore, be neglected in studies of pulsar evolution in the  $P-\dot{P}$  diagram, birthrate studies, *etc.* This, coupled with the injection which we have demonstrated, would cast doubts on earlier analyses of pulsar data. A complete re-examination is called for.

(d) The mean braking index of pulsars is estimated to be  $3.7_{-0.8}^{+0.8}$  this value being probably an overestimate. Hence the dipole braking model value of  $n = 3$  is probably close to the truth. Also,  $\tau = \frac{1}{2}P/\dot{P}$  appears to be a good indicator of pulsar age upto  $6 \times 10^6$  yr, which might be a lower limit for the decay time of the magnetic field or possibly the age at which pulsars begin dying. These results do not depend upon our choice of  $K$  and  $n_e$ .

### Acknowledgements

We are thankful to Rajaram Nityananda for numerous helpful discussions and suggestions, to V. Radhakrishnan for suggesting the possibility of injection, to J. H. Taylor for drawing our attention to the importance of luminosity selection effects, and to R. N. Manchester for providing in preprint form half of the data that we have used in this analysis. We also thank both our referees for many valuable suggestions.

### Appendix A

In various sections of this paper, we are interested in evaluating quantities of the form

$$Q = \int x p(x) dx \quad (32)$$

where  $x$  is some property of pulsars and  $p(x) dx$  is the probability of observing a pulsar having a value of this property in the range  $x$  to  $x + dx$ . For instance, in Section 2(b),  $x = \dot{P}S(L)$ , in Section 2.4,  $x = S(L)$ , *etc.* We estimate  $Q$  by means of the following sum over the  $X_i$  of the observed pulsars

$$Q_{\text{est}} = \sum_{i=1}^N X_i. \quad (33)$$

Now, the probabilities of observing pulsars in different ranges of  $x$  are independent of one another. Hence,  $Q$  in equation (32) is the weighted integral over independent Poisson variables (of mean  $p(x) dx$ ). The variance of  $Q$  is then clearly given by

$$V = \int x^2 p(x) dx. \quad (34)$$

This can be estimated in terms of the observed pulsars by means of

$$V_{\text{est}} = \sum_{i=1}^N X_i^2 \quad (35)$$

which is the formula used throughout the present paper.

The form of  $V$  in equation (34) is different from the following more usual form

$$\begin{aligned} V' &= \int (x - \bar{x})^2 p(x) dx \\ &= \int x^2 p(x) dx - \bar{x}^2 \int p(x) dx \end{aligned} \quad (36)$$

The difference arises because the variance in the present case (equation 34) has two contributions.

(a) There is one contribution arising from the distribution of values of  $x$ , giving an expression exactly of the form equation (36).

(b) Secondly, being a Poisson process, the total number of observed pulsars

$$N = \int p(x) dx \quad (37)$$

can itself fluctuate *i.e.* there can be fluctuations in the number of terms in equation (33). It is easily verified that this contribution cancels the second term in equation (36), leading to equation (34).

## Appendix B

If an H II region lies along the line of sight to a pulsar, it contributes to the dispersion measure (DM). Since pulsar distances are derived using DM, the H II region contributions must be subtracted. Prentice and ter Haar (1969) have given a scheme for estimating the corrections. However, their results might be inaccurate because of unknown parameters, such as the Strömgren radii and electron densities of the H II regions. The inaccuracies could be particularly serious if the H II region contribution is a major fraction of the pulsar's DM. Therefore, we have 'softened' the Prentice-ter Haar correction using the following scheme.

We postulate that the dispersion measure correction of an H II region has a rectangular probability distribution as shown in Fig. 7 where  $H$  is the correction given by Prentice and ter Haar. We average the calculated distance to the pulsar over this probability distribution and use the averaged distance in our studies. Let  $d$  be the

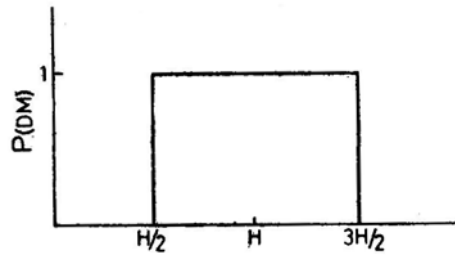


**Figure 7.** Assumed probability distribution of the dispersion measure correction ( $H$ ) due to H II regions.

DM left to be accounted for just at the front face of the H II regions. It is easy to see that whenever  $d \geq 3H/2$  or  $d \leq H/2$ , the present scheme gives practically the same distance as the old scheme (which directly used the single value of  $H$ ). For the case  $H/2 < d < 3H/2$ , the new scheme gives a larger estimate for the pulsar distance than the old. A larger distance implies a larger estimate for the pulsar luminosity  $L$  and hence a smaller estimate of the scale factor  $S(L)$ . We are thus, in a sense, being conservative and erring on the side of slightly underestimating the quantities of interest.

### Appendix C

As already mentioned in the text, we expect the distribution of  $Q_{\text{est}}$  (equation 33) to be asymmetric, with a long tail, because only a few top values of  $X_i$  usually contribute to the result. Therefore we prefer to use confidence limits rather than the Standard deviation. In computing the confidence limits, we assume that our estimator

$Q_{\text{est}} = \sum_{i=1}^N X_i$  is the sum of  $N$  random Poisson variables ( $v_i$ ) of mean equal to 1, each weighted by the respective  $X_i$

$$Q_{\text{est}} = \sum_{i=1}^N v_i X_i. \quad (37)$$

By numerically generating  $N$  random variables between 0 and 1, we generate  $N$  random Poisson variables with mean 1 and therefore a random value of  $Q_{\text{est}}$ . By generating many random values of  $Q_{\text{est}}$ , we then estimate the probability distribution of  $Q$ . The confidence limits are then easily marked off by measuring areas under this probability curve.

### References

- Arnett, W. D., Lerche, I. 1981, *Astr. Astrophys.*, **95**, 308.  
 Baade, W., Zwicky, F. 1934, *Proc. nat. Acad. Sci.*, **20**, 254.  
 Clark, D. H., Caswell, J. L. 1976, *Mon. Not. R. astr. Soc.*, **174**, 267.  
 Clark, D. H., Stephenson, F. R. 1977, *Mon. Not. R. astr. Soc.*, **179**, 89p.  
 Davies, J. G., Lyne, A. G., Seiradakis, J. H. 1972, *Nature*, **240**, 229.  
 Davies, J. G., Lyne, A. G., Seiradakis, J. H. 1973, *Nature Phys. Sci.*, **244**, 84.  
 Davies, J. G., Lyne, A. G., Seiradakis, J. H. 1977, *Mon. Not. Roy. astr. Soc.*, **179**, 635.

- de Loore, C., de Greve, J. P., de Cuyper, J. P. 1975, *Astrophys. Sp. Sci.*, **36**, 219.
- Downes, D. 1971, *Astr. J.*, **76**, 305.
- Gold, T., 1968, *Nature*, **218**, 731.
- Groth, E. J., 1975, *Astrophys. J. Suppl. Ser.*, **29**, 453.
- Hulse, R. A., Taylor, J. H. 1974, *Astrophys. J.*, **191**, L 59.
- Hulse, R. A., Taylor, J. H. 1975, *Astrophys. J.*, **201**, L 55.
- Illovaisky, S. A., Lequeux, J. 1972, *Astr. Astrophys.*, **20**, 347.
- Katgert, P., Oort, J. H. 1967, *Bull. astr. Inst. Netherl.*, **19**, 239.
- Kundt, W. 1981, *Nature*, **292**, 865.
- Lyne, A. G., Ritchings, R. T., Smith, F. G. 1975, *Mon. Not. Roy. astr. Soc.*, **171**, 579.
- Manchester, R. N., Taylor, J. H. 1977, *Pulsars*, Freeman, San Francisco.
- Manchester, R. N., Lyne, A. G., Taylor, J. H., Durdin, J. M., Large, M. I., Little, A. G. 1978, *Mon. Not. R. astr. Soc.*, **185**, 409.
- Manchester, R. N. 1979, *Austr. J. Phys.* **32**, 1.
- Milne, D. K. 1970, *Austr. J. Phys.*, **23**, 425.
- Narayan, R., Vivekanand, M. 1981, *Nature*, **290**, 571.
- Ostriker, J. P., Gunn, J. E., 1969, *Astrophys. J.*, **157**, 1395.
- Phinney, E. S., Blandford, R. D. 1981, *Mon. Not. R. astr. Soc.*, **194**, 137.
- Poveda, A., Woltzer, L., 1968, *Astr. J.*, **73**, 65.
- Prentice, A. J. R., ter Haar, D. 1969, *Mon. Not. R. astr. Soc.*, **146**, 423.
- Radhakrishnan, V. 1981, *Preprint*.
- Ritchings, R. T. 1976, *Mon. Not. R. astr. Soc.* **176**, 249.
- Srinivasan, G., Dwarakanath, K. S. 1981, *Preprint*.
- Tammann, G. A. 1974, in *Supernovae and Supernova Remnants*, Ed. C. B. Cosmovici, D. Reidel, Dordrecht.
- Tammann, G. A. 1977, *Ann. N.Y. Acad. Sci.*, **302**, 61.
- Taylor, J. H., Manchester, R. N. 1977, *Astrophys. J.*, **215**, 885.
- van den Heuvel, E. P. J. 1977, *Ann. N.Y. Acad. Sci.* **302**, 14.
- Zwicky, F. 1962, in *IAU Symp. 15; Problems of Extragalactic Research*, Ed. G. C. Mevittie, Macmillan, New York.